# Metallurgical aspects in grind-hardening of heat treatable steels

H.A.A. Youssef and M.Y. Al-Makky
*Production Eng. Dept., Faculty of Eng., Alexandria University, Alexandria, Egypt*

Grind-Hardening (GH) is a new promising surface strengthening technology suggested by Brinksmeier, IWT-Bremen University. It is an integrated process comprising machining and surface hardening performed simultaneously in one step by utilizing the heat flux of machining in order to exert the intended surface hardening, thus realizing both economical and ecological advantages. However, Grind-Hardening is not well established as a competing surface hardening process due to lack of information regarding the effect of the unlimited number of parameters that influence the results of this process. For that reason intensive research on this topic should be systematically carried out at different operational parameters on the applicable type of heat treatable steels. This paper is a trial to do this, considering Grind-Hardening as a metallurgical problem. The TTT-diagrams of investigated steels are hereby considered to study the phase-transformations that occur in what is called Heat Treated Zone (HTZ), under the prevailing cooling rates.

التجليخ التصليدى Grind-Hardening هى تكنولوجيا جديدة واعدة من تكنولوجيات تقسية السطوح بغرض تقويتها، والتى اقترحها Brinksmeier, IWT, Bremen Univ. وتُعرف الطريقة على أنها عملية تكاملية integrated process تتألف من التجليخ مع استخدام حرارته آنياً فى تقسية سطح الشغلة الحديدية، وبذلك تتحقق ميزة اقتصادية وأخرى بيئية نتيجة هذا التكامل. غير أن هذه العملية يعتريها نقص كبير فى البيانات الخاصة بتأثير العدد اللامحدود من المتغيرات على نتائج هذه العملية، يجعلها قاصرة حتى الآن عن التطبيق. لذلك يجدر القيام ببحوث لدراسة عملية التجليخ التصليدى من منظور ميتالوجرافى لتحديد التحولات البللورية فى منطقة المعالجة الحرارية HTZ على سطح الشغلة عند معدلات التبريد المختلفة، على أن تجرى هذه الدراسة على الأنواع المختلفة من الصلب والصلب السبائكى، المستخدمة بكثرة فى مختلف التطبيقات الصناعية.

**Keywords:** Grind-hardening, Surface integrity, Heat treated zone

## 1. Process development

During grinding, almost the whole mechanical energy induced at the surface of the wheel and workpiece dissipates into thermal energy. The generation of imperfections due to the associated thermal effect is a well-known problem. Such imperfections do affect the surface integrity of ground components [1]. Many scientists investigated the metallurgical damage due to the grinding burn in the so called Heat-Affected-Zone (HAZ) when grinding steels [2-5].

Wagner in 1957 defined for the first time grinding as “an unintentional heat treatment process.” [6]. However, recent research results indicated that the thermal energy may be utilized intentionally for heat treatment purposes, and hence a new technology has been suggested by Brinksmeier [7] in 1994. It is called Grind-Hardening or Hardening by Grinding,. It is “an integrated machining/heat treatment method, aiming at strengthening of the surface layer of components”.

It is well established now that Grind-Hardening process utilizes the heat flux generated mainly at abusive grinding conditions to induce controlled martensitic phase transformation in the workpiece shell of annealed or tempered steels. The Grind-Hardening process is characterized by high grinding forces, excessive wheel wear, and high surface roughnesses, making necessary sometimes to perform finishing process after Grind-Hardening to enhance the surface integrity properties of the ground components [2, 8]. Fig. 1 shows the principle of Grind-Hardening of heat treatable steel, as well as the hardness and the residual stress profile of a ground-hardened surface [8].

Grind-Hardening is basically a dry grinding process. The application of coolants and lubricants as chilling elements is not essential, because the critical cooling rate is

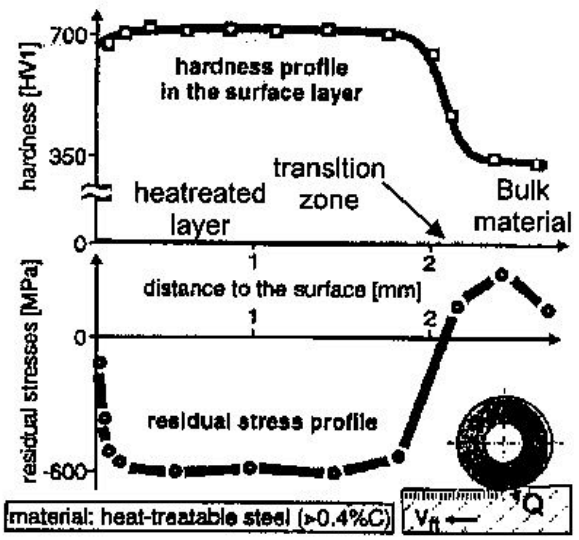


Fig.1. Hardness and residual stress profiles associated in Grind-Hardening [8].

reached by the self-quenching nature of the workpiece material. An important aspect of Grind-Hardening is its environmental considerations and its legal implication; moreover, there is no need for the environmentally non-friendly heat treatment appliances.

Grind-Hardening can therefore be classified as a rapid surface strengthening process [1], which is characterized by the combined thermomechanical alteration of the surface layer. Due to the mechanical effect exerted by the grinding wheel, the metallurgic transformation does not need long time to occur, and it could be performed in one pass of the grinding wheel, which lasts only a fraction of a second. Consequently Grind-Hardening is a short-time process and proved to be productive as compared to strengthening methods based on both thermochemical and mechanical mechanisms. However, it should be considered that the mechanical strengthening methods are suitable for all types of metals, ferrous and non-ferrous, whereas other methods, including Grind-Hardening are only applicable for heat treatable steels. The achievable strengthening depth by Grind-Hardening is comparable with those achieved by other surface hardening methods.

Moreover, Grind-Hardening realizes economical benefits due to its increased integration levels [4]. By adopting Grind-Hardening as a new heat treatment method, both hardening and grinding can be combined in one step leading to shortened process sequence and less transportation [9]. Grind-Hardening can specially be used for manufacturing components which are subjected to medium or low operating impact loads and just need a hardness penetration of a few tenths of millimeter to improve their wear resistance. Grooves for locking rings, guide ways, gear box levers, and threads of packing rings, are some examples [9, 10].

## 2. Grind-hardening and associated phase-transformations

The hardening process of heat treatable steels depends mainly upon their chemical composition, carbon and alloying element contents, as well as their pre-heat treatment conditions.

The transformations that occur due to the thermomechanical mechanism in Grind-Hardening are more complex than those occurring in conventional hardening, since these are associated with relatively short times at elevated temperature before quenching. The significance of short-times at high temperature in grinding, is not associated with the time required for the ferrite-austenite $\alpha$-$\gamma$ transformation, but rather with the time required for decomposition of carbides and homogenization of carbon $C$ in $\gamma$ before quenching [2].

Before considering the short-time Grind-Hardening mechanism, the conventional hardening process should be at first highlightened through some metallurgical fundamentals.

### *2.1. Metallurgical considerations in conventional hardening*

- It is well established, that plain carbon steels with less than 0.3% $C$ cannot be effectively hardened. Hardness increases with increasing carbon up to about RC=66 (HV0.5= 960) at 0.6% $C$ [12]. For more increase of carbon content, the hardness does no increase due to the formation of retained austenite in high carbon steels. The proportion of retained austenite increases from 1% to 15% if the

carbon content in steel increases from 0.4% *C* to 1.2% *C*, fig 2-b [13]. It is well known that the retained austenite is reduced by subzero quenching.

- The hardenability and, hence, the grind-hardenability of steels are greatly affected by additions of alloying elements, eventhough if these additions are in small quantities as in low alloy steels. The following equation expresses the so-called equivalent carbon content, *C-eqt.*, which is considered as a reliable measure of the hardenability of heat treatable alloy steels.

$$C\text{-}eqt. = C\% + \frac{(Cr+Mo+V)}{5}\% + \frac{(Mn)}{6}\% + \frac{(Cu+Ni)}{15}\%$$

- The hardening mechanism, as based on the $\alpha/\gamma$ transformation during heating, begins at the critical temperature $A_1$ (706°C), and is completed on crossing the line $A_3$, and even exceeding it by about 50°C, fig 2-a [13]. Long soaking for an hour or more may be necessary for carbon to be uniformly diffused or dissolved in $\gamma$. The steel is then rapidly quenched at a rate ranging from 10 to 500°C/s, depending on alloying element contents. The quenching must exceed the critical cooling rate to allow martensitic transformation to occur, which begins at certain temperature $M_s$ and terminates at a temperature $M_f$, fig. 2-b.

The value of $M_s$ is affected by the alloying elements according to the following empirical formula, provided that all carbides have been dissolved in the austenite $\gamma$ [14].

$$M_s = 520 - 320\%C - 50\%\ Mn - 30\%\ Cr - 20\%\ (Ni + Mo) - 5\%\ (Cu + Si)\ \ ^\circ C$$

Fig. 2-c demonstrates also the martensite curve and the retained austenite of 5% for a pearlitic plain carbon steel.

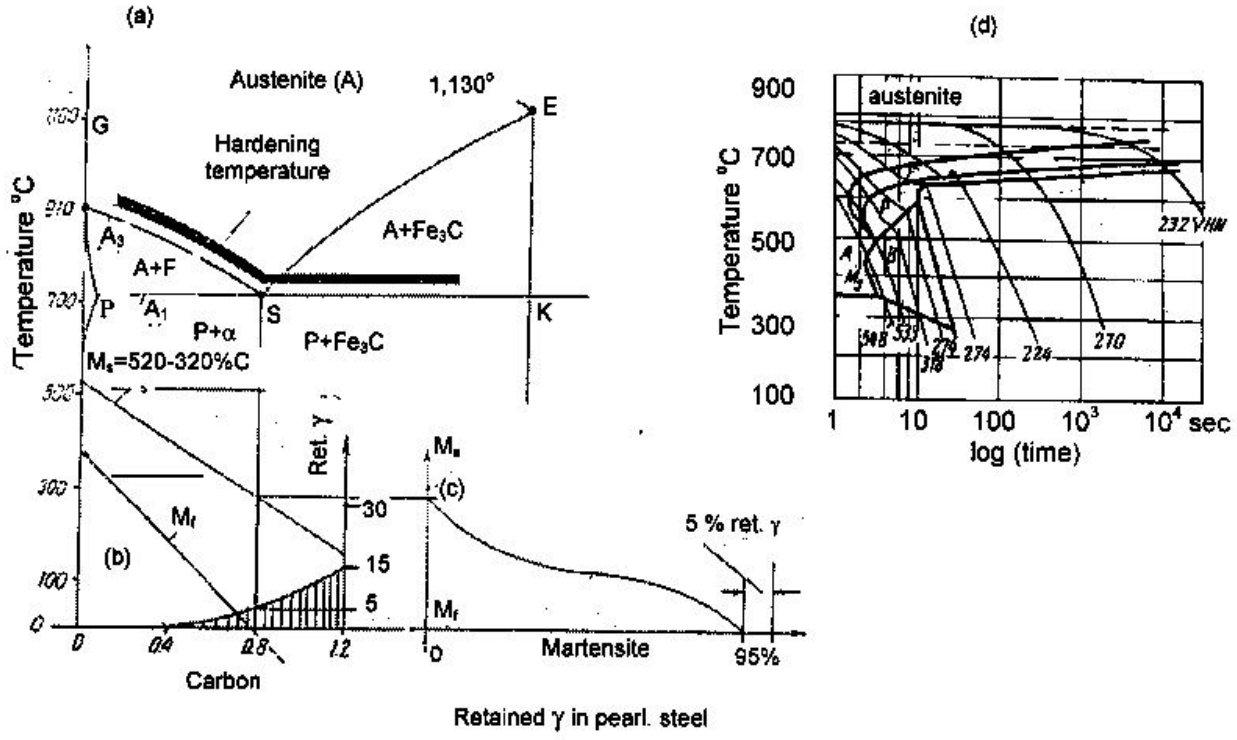


Fig. 2. a- Hardening temperature of hypo-and hypereutectoid plain carbon steels
b- Effect of carbon content on Ms, Mf, and retained Austenite
c- Martensite and retained autenite for a pearletic plain carbon steel
d- TTT-diagram of plain carbon steel of 0.45%C [13].

- The time-temperature-transformation TTT-diagrams, also called C-curves are most useful in presenting an overall picture of the austenitic transformation. The decomposition of austenite results, depending on the cooling rate, in three different main products: Pearlite P, Bainite B, and Martensite M.

Fig. 2-d [13], shows the TTT-diagram of the plain carbon steel 0.45%C. Different cooling curves are shown on the same diagram. The most rapid cooling curve is the first from the left. Referring to fig. 2-d, martensitic transformation starts at $M_s$= 370°C and terminates at $M_f$ = 150°C with negligible amount of retained austenite, see also fig. 2-b.

Common alloying elements except Co can cause the TTT-diagram to be displaced to the right, fig. 3-a [12]. In other words, alloying elements make the formation of martensite to take place at slow speeds of cooling, provided that, they should be in solid solution in $\gamma$ before quenching. If the carbide forming alloying elements such as *Cr*, *Mo*, *W*, *Mn*,…, are present as insoluble stable carbides [(Fe, *Cr*)$_3$ *C*, (*Fe*, *Mo*)$_3$ *C*,….], they may actually shift the TTT-diagram to the left such that higher cooling rates are needed for martensite formation.

The effect of grain growth of austenite on the hardenability is schematically shown in fig. 3-b. The finer the austenite grain size, the further the TTT-diagram is placed to the left. Hence, a fine-grained steel must be cooled more quickly than a coarse grained steel if the formation of pearlite and bainite is to be avoided.

Fig. 4, demonstrates the effect of temperature and carbon content on the austenite grain growth [13]. The soaking time has also a great effect on the austenite grain growth at a constant temperature.

- The ternary system is used to estimate the eutectoid point and the critical temperatures $A_1$, and $A_3$ for alloy steels. Fig. (5) shows the *Fe-C-Cr* ternary system, from which it is depicted that *Cr* (also *W, Mo, Si*,…) narrows the $\gamma$-phase range. It gradually encloses the $\gamma$ range and shifts the points S and E to the left. It also raises the eutecoid points S to higher temperature values.

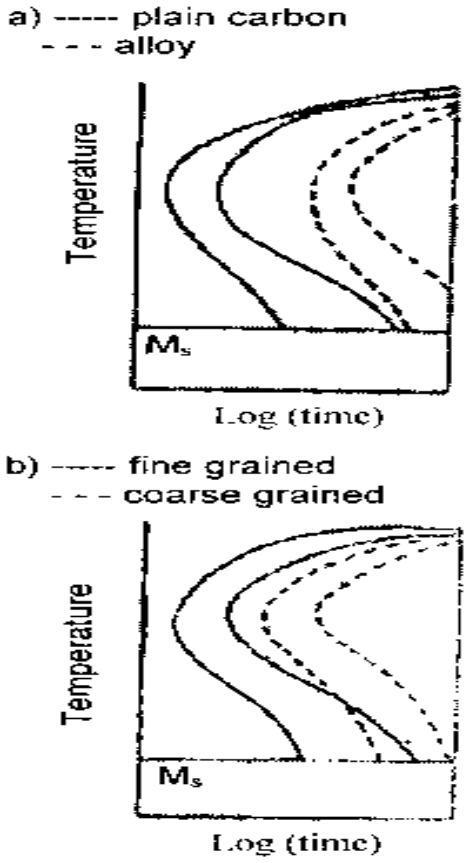


Fig. 3. Shifting of TTT-diagrams due to a) allowing elements, b) grain size.

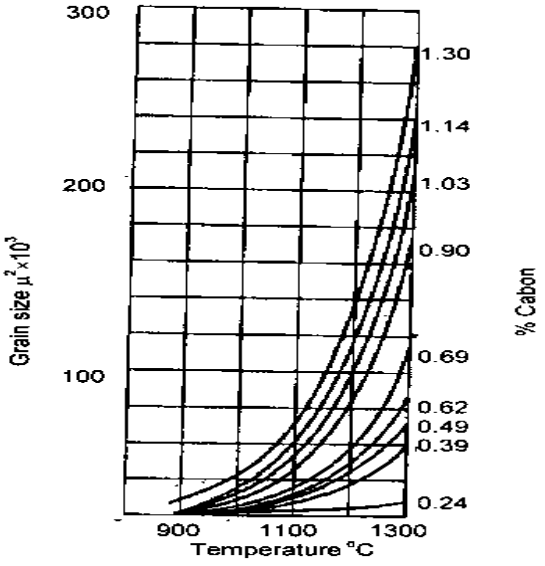


Fig. 4. Effect of temperature and carbon content on the-$\gamma$ grain size of plain carbon steels [13].

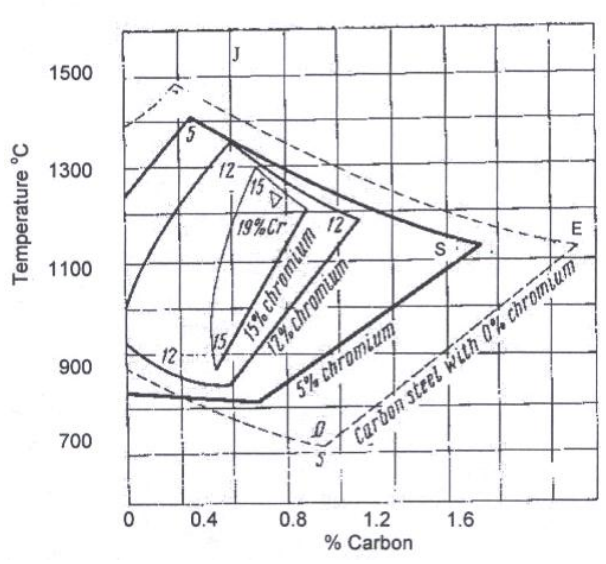


Fig. 5. Fe-C-Cr ternary system indicating the $\gamma$-phase range of the alloy steels 42CrMo4 (1%Cr) and 100 Cr6 (1.5% Cr) found by interpolation [13].

*2.2. Short-time grind-hardening mechanism*

One of the main advantages of short-time Grind-Hardening is that the austenitic grain growth is totally eliminated. As said before, the short-time heating is not significant as concerned with $\alpha$-$\gamma$ transformation, if the critical cooling rate needed for martensitic transformation is reached [2, 10-11]. The cooling is only affected by self-quenching of the surface layer by the cooler workpiece core. So the cooling rate depends on the material property and geometrical characteristics of the machined workpiece.

*2.2.1. Thermal model and recommended grinding parameters in surface down -cut plunge grind-hardening*

*2.2.1.1. $\alpha$-$\gamma$ transformation (short-time heating)*
The grinding energy is dissipated as heat out the rectangular grinding zone of length $l_c$ and grinding width b, during grinding pass along workpiece length $l_w$. The arc of contact $l_c$ is decisively influenced by the wheel diameter $d_s$ and the depth of cut a, according to eq. (1)

$$l_c = (a.d_s/2)^{0.5} . \quad (1)$$

The heat input to the workpiece can be linked to a triangular distribution of continuous heat source, which moves along the surface at the workspeed $v_w$, fig. 6 [12, 15-16].

Therefore, the heating time $t_h$ in this case is given by:

$$t_h = l_c/v_w . \quad (2)$$

For the most cases $t_h$ is estimated as a fraction of a second. It is well established that the heating time required for $\alpha$-$\gamma$ reaction (and also the cooling time required for $\gamma$-$\alpha$ reaction) is extremely short, in the order of 0.1 $\mu$s [17]. Therefore why is a long heating (soaking) time required in case of conventional heat treatment. The answer is that the prolonged time in conventional treatment is necessary for carbides to dissolve and diffuse into the $\gamma$ unit cell in order to be homogenized [2]. On the other hand, the matrix $\gamma$ in case of Grind-Hardening is not stationary as in conventional hardening, but is being plastically deformed at a very high-rate during grinding, such that short-time, fraction of a second, is more than sufficient for diffusion of carbides in $\gamma$ to occur [2].

The surface temperature $\theta s$ to provide a given layer thickness $y$ (cm) of untempered martensite (UTM) is given by eq. (3) [18].

$$\theta s/\theta y = 1/1 - erf \frac{y}{2\sqrt{\alpha t_h}}, \quad (3)$$

where:
$\theta y$ is the temperature at a distance y from the surface,
$\alpha$ is the thermal diffusivity of work (steel) = 0.127 cm$^2$/s, and
*erf* is the Guassian error function.

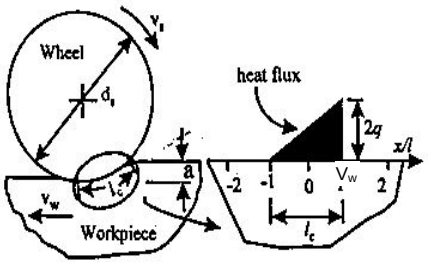


Fig. 6. Thermal model in surface-plunge Grind-Hardening [16].

*2.2.1.2. Recommended working parameters for Grind-Hardening* The generated heat quantity during Grind-Hardening, and consequently the achievable austenitizing depth, depends more or less on the grinding parameters. These correlations are rather complex and not yet totally clarified. However, to achieve good results in Grind-Hardening, it is recommended to select high depths of cut (a= 1mm), and medium feed rates ($V_w$= 0.1-1 m/min). No general valid interrelation between $V_s$ and hardening results has been detected [9]. Resin bonded grinding wheels give the best hardening results due to their low thermal conductivity. In Grind-Hardening cooling has no relevance [9]. However, dry grinding is still considered the ultimate goal [1].

Tempered steels are highly recommended for Grind-Hardening, where better results are achieved more than if annealed steels are used. In grinding hardened steels, the thermo-mechanical load causes undesired damage in the surface layer, like cracks, over-tempered zones and White Etching Areas (WEA). These effects were known for a long time and are thoroughly investigated [2, 4, 20]. For that reason, hardened steels are not recommended for Grind-Hardening [1, 2, 20].

*2.2.1.3. γ- Martensitic transformation (self-quenching)* Rapid self-quenching of the already formed austenitic layer during Grind-Hadening may exceed 100°C/s. It secures in the most cases, the formation of martensitic structure, specially in case of alloy steels.

*2.2.2.Grind-Hardening of hypoeutecoid and hypereutocoid alloy steels*

Brinksmeier and Brockhoff [11], examined the Grind-Hardening of two types of alloy steels, namely the hypoeutecoid alloy steel 42*CrMo*4, and the hypereutecoid ball bearing steel 100*Cr*6. The chemical compositions as well as the carbon equivalents of both steels are given in table 1.

Fig. 7 shows in comparison the hardness distribution HV0.5 in the so-called Heat Treated Zone (HTZ) as a function of the depth beneath the work surface for both alloy steels, as well as the resulting microstructures [11]. The grinding conditions are given in the same figure.

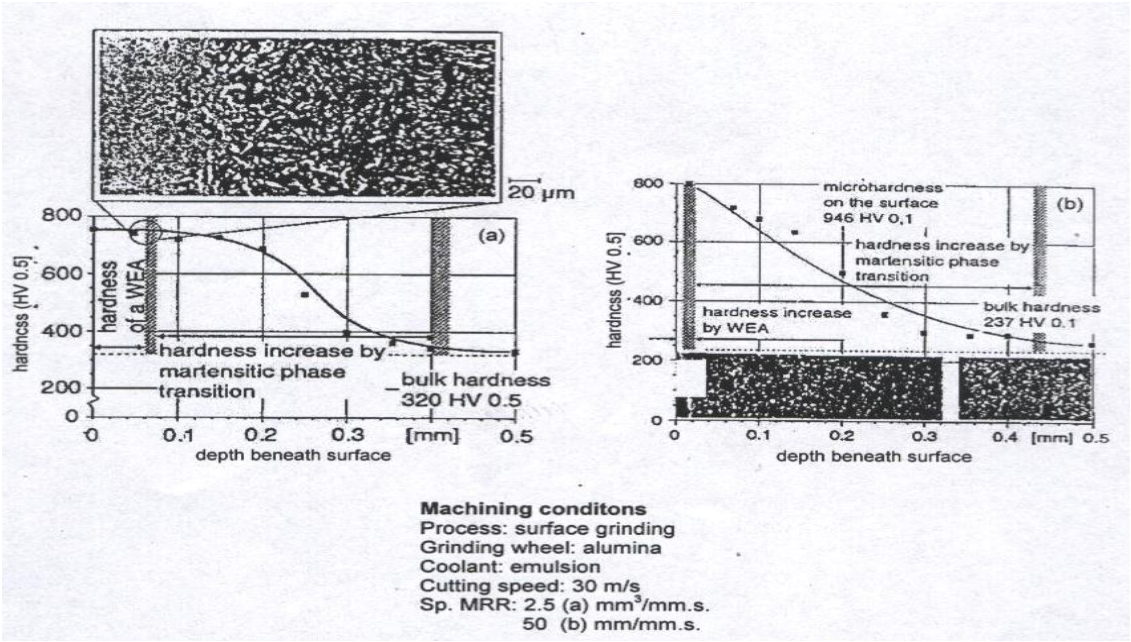


Fig. 7. Hardness distribution HV 0.5 in the HTZ in comparison for the hyoeutectoid steel (a) 42 *CrMo4* and the hypereutectoid steel (b) 100 *Cr6* as well as the related micro-structures, according to Brinksmeier and Brockhoff [11].

Table 1
Chemical composition of 42 *CrMo*4 and 100 *Cr*6 alloy steels

| DIN | Chemical composition | | | | | | | C-Equiv. |
|---|---|---|---|---|---|---|---|---|
| | *C* | *Si* | *Mn* | P+S% | *Cr* | *Mo* | *Ni* | |
| 42CrMo4 | 0.38-0.45 | 0.15-0.35 | 0.75 | <0.06 | 0.9-1.2 | 0.15-0.3 | - | 0.75 |
| 100Cr 6 | 0.9-1.05 | 0.3 | 1.35 | <0.06 | 1.35-1.65 | - | <0.3 | 1.35 |

According to their results, fig 7-a, the hardness distribution in case of hypoeutecoid tempered steel 42CrMo4 shows a distinct plateau at 750HV0.5, with a WEA starting from the surface to a depth of 60µm followed by martensitic structure down to a depth of 200µm from the surface. Then the hardness decreases continuously to the hardness of bulk tempered structure of 320HV0.5. The whole HTZ covers 350-400µm, and the whole structure is composed of etchable martensite. Moreover, the Grind-Hardening of tempered steels can be achieved at relatively soft grinding condition using a spec. removal rate $Q'w$= 2.5 mm$^3$/mm s [11]. Fig. 7-b shows the hardness distribution after Grind-Hardening under abusive working conditions of the annealed bearing steel 100 Cr 6. The depths of the HTZ beneath the surface is about 300µm, [4]. The HTZ in this case is composed of two different layers. Directly at the surface, an extra hard WEA is generated within 20µm, followed by a hard structure consisting of matensite and carbides, [11]. In this case, high spec. removal rate of $Q'w$ = 50mm$^3$/mm s is selected to induce martensite phase transformation of the annealed hypereutecoid steel 100Cr6.

Based on the experimental results of Brinksmeier and Brockhoff [11], the Grind-Hardening process of both alloy steels 42*CrMo*4 and 100 *Cr*6 is reconsidered with special emphasize to metallurgical fundamentals proceeded. Both steels 42CrMo4 and 100 Cr6 as demonstrated on ternary system, fig. 5, are categorized as low *Cr*-alloy steels. Other alloying element existing in both steels are considered insignificant as concerned with their equilibrium diagrams. Fig. 8 demonstrates the equilibrium diagrams of both steels, whereas table 2 visualizes their eutecoid points S, critical temperatures, hardening temperature and martensite transformation temperatures $M_s$ and $M_f$.

Table 2
Eutectoid points S, critical temperatures $A_1$, $A_3$ and Martensite Transformation temperatures $M_s$, $M_f$ of both steels 42 *Cr Mo*4 and 100 *Cr* 6

| Steel | 42 *Cr Mo* 4 | 100 *Cr 6* |
|---|---|---|
| Eutectoid points S | 0.73 | 0.70 |
| Low/ upper critical temp. | 735/800 | 750/860 |
| Hardening temp. | 800 °C | 860 °C |
| Martensite transf. temp. | | |
| $M_s$ | 340 °C | 245 °C |
| $M_f$ | 120 °C | 35 °C |

The correlation between the cooling rates and the microstructure as expected has been thoroughly investigated considering the hardness distribution according to [11], and the TTT-diagrams of both steels.

### *2.2.2.1. Grind-Hardening of the hypoeutecoid tempered alloy steel 42CrMo4*

When the alloy steel 42*CrMo*4 is heated to the austenitizing temperature 820-870°C, phase transformation ($\alpha$ + P $\rightarrow\gamma$) is allowed to take place. Two factors enhance the diffusion of carbon atoms in austenite; these are the high rate of plastic deformation during grinding, and the fine grain size of the tempered steel. However, due to the short heating time, sufficient homogenity of carbon (carbides) in $\gamma$ may not be realized.

Fig. 9-a shows the TTT-diagram of the alloy steel 42*CrMo*4 with cooling curves superimposed [12]. The hardenability of this steel is enhanced by the addition of alloying elements as this diagram is shifted to the right as compared with that of the plain carbon steel of the same carbon content, fig. 3-a.

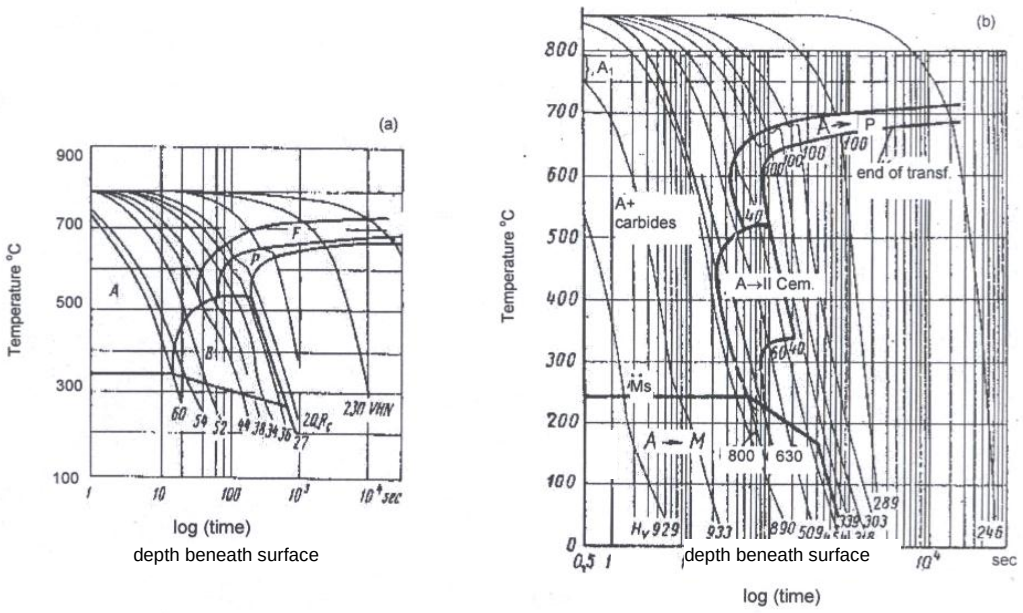


Fig. 8. The TTT-diagrams with cooling curves super-improved for, a) hypoeutectoid steel 42 *CrMo*4 [13]
b) hypereutectoid steel 100 *Cr6* [21].

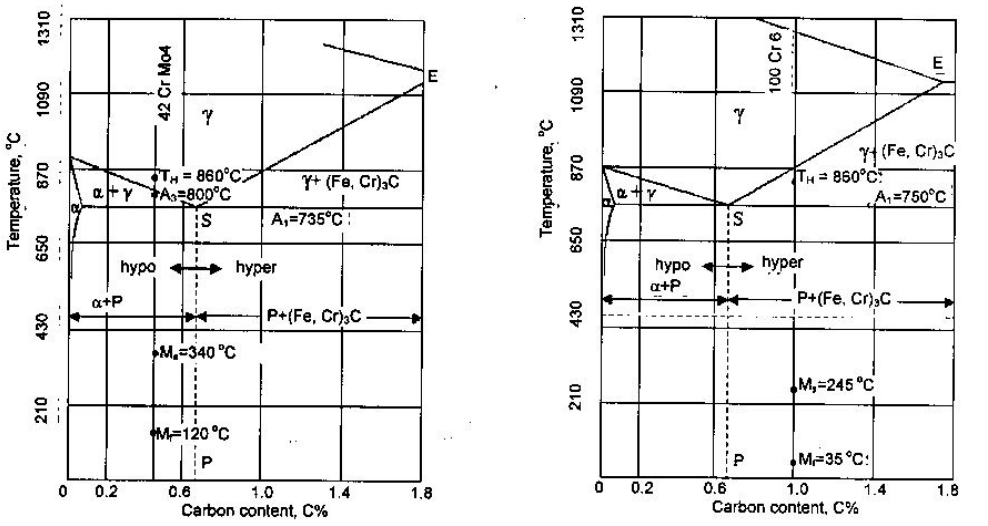


**Eutectoid point S:**0.73%C, (Pearlitic),
P = α+ (Fe, Cr)$_3$C
**Critical points:** $A_1$=735 °C, $A_3$= 800 °C
**Hardening:**
Short-time heating to 860 °C,
α + P → γ
Self-quenching for martensitic trasformation on surface,
γ → bct (martensite)
$M_s/M_f$=340 °C/120 °C

**Eutectoid point S:** 0.7%C, (Pearlitic), P = α+ (Fe, Cr)$_3$C
**Critical points:** $A_1$=750 °C, $A_3$=860 °C
**Hardening:**
Short-time heating to 860 °C,
P+ (Fe, Cr)$_3$C → γ +(Fe , Cr)$_3$C
Self-quenching for martensitic trasformation on surface, γ + (Fe,Cr)$_3$C
M+(Fe , Cr)$_3$C + Retained γ
$M_s/M_f$ =245 °C/35 °C

Fig. 9. a- Equil. diagram of hypoeutectoid steel 42 *Cr Mo* 4
b- Equil. diagram of hypoeutectoid steel 100 *Cr* 4.

The TTT-diagram Fig. 9-a describes how the austenite is decomposed depending on the cooling rates. Referring to the TTT-diagram fig. 10 illustrates the estimated mean cooling rates, as based on the achieved hardness and the expected microstructure within the HTZ. If the cooling rate, 1st cooling curve, fig. 9-a, exceeds the critical rate (32°C/s), a white etchable area (WEA) of 60μm beneath the surface is formed, which is composed of cementite dispersed in martensite matrix at the surface. At critical cooling rate, 2nd cooling curve fig. 9-a, martensitic transformation occurs achieving a hardness of 60 RC (750 HV0.5), in a zone at a depth between 60 μm and 150μm beneath the surface.

When moving towards the core, cooling rates of 22, 9.5, 2.5°C/s [corresponding to 3rd, 4th, and 5th curve, fig. 9-a] predominate such that martensitic/bainitic microstructure forms between depths of 150μm and 300μm. At very low cooling rate of 0.75°C/s [corresponding to the 8th cooling curve, fig. 9-a], the austenite is decomposed in $\alpha$+fine pearletic structure at depths between 300 to 400μm, after which the bulk material 42*CrMo*4 with hardness of 320HV0.5 (33 RC) is existing, fig. 10-a. The finess and hardness of structure increase as the surface is approached.

Therefore, the HTZ of this steel is about 400μm and the hardness shows a distinct plateau of 750HV0.5 for a depth 150μm beneath the surface, fig. 10-a.

*2.2.2.2. Grind-Hardening of the hypereutecoid annealed alloy steel 100 Cr6*

In hypereutecoid steels full diffusion of cementite $(Fe, Cr)_3 C$ is not recommended, fig. 2-a. The autenitization is carried out below the ES line to avoid unhealthy grain growth. fig. 8-b.

Fig. 9-b shows the TTT-diagram of the annealed steel 100*Cr*6 with cooling curves of different rates. The hardenability of this steel is greater than that of 42*CrMo*4, since the TTT-diagram is somewhat shifted to the right and so it permits the martensitic transformation to occur at relatively lower critical cooling speed (22°C/s). Moreover, the steel 100*Cr6* has a higher *C-eqt.* as compared with the steel 42*CrMo4*, table 1.

Fig. 10-b shows the estimated mean cooling rates, as based on the achieved hardness in the HTZ, and the corresponding microstructure.

Due to the self-quenching, the surface of the workpiece is subjected to a cooling rate (3rd curve in the TTT-diagram, fig. 9-b greater than critical cooling rate, such that martensitic transformation takes place, and a WEA, composed of martensite and carbides is formed. At a depth of 20μm beneath the surface, the critical cooling rate of 22°C/s is affected, where a hardness of 800 HV0.5 (62RC) is achieved in a thin layer from 20 to 60μm of martensite, carbides and retained austenite. The amount of retained austenite increases due to the presence of *C* (1%) and *Cr*(1.5%) in the investigated hypereutecoid steel 100*Cr6*.

A layer of M + B + Cem. + ret $\gamma$, formed between 60 and 120 μm of hardness ranging from 720 to 630 HV0.5. It is achieved at cooling rates from 20 to 11°C/s. At lower cooling rates from 11 to 4°C/s, the microstructure is composed of B + Cem. At the smallest cooling rates from 2 to 0.4°C/s, fine to coarse pearlite+Cem. is formed, fig. 9-b. The total HTZ is accordingly 300μm with no evidence of clear hardness plateau, fig. 10-b.

## 3. Concluding remarks

- Grind-Hardening functionally differs from grinding in that it is performed under severe working conditions, where the work material must be heat treatable steel, while grinding is a machining operation, which is performed under moderate and soft working conditions and it is dedicated to machine all types of materials, metallic or non-metallic. The surface integrity is greatly impaired by Grind-Hardening rather than grinding.
- Grind-Hardening operation should be treated as a metallurgical problem. The TTT-diagram of the heat treatable steel should be considered to predict and control the depth and the microstructure of the surface layer. As a matter of fact, the cooling rates during self-quenching should be more precisely determined.
- One of the advantages of the Grind-Hardening is being a rapid surface strengthen-

ing operation. Due to the short heating time, the grain growth of austenite is hampered, and the carbides have no chance to dissolve as compared with conventional hardening, leading to appreciable strength, toughness and hardness of the micro-structure.

- Pre-hardened steels should not be considered for Grind-Hardening, whereas tempered pre-heated steels are best suited to be grind-hardened.
- If possible, pilot tests for checking grind-hardenability may be recommended. The test should be performed on the same type of pre-treated steel under the same parametric conditions.
- After Grind-Hardening, it is a good practice to adopt a finish cut to improve the surface integrity and hence enhancing the fatigue strength, by removing the WEA from the part surface. The condition of finishing cut should be carefully selected, (it may be a number of sparking out strokes). Only a small amount of heat flux is required to temper the martensitic structure of HTZ, properly.

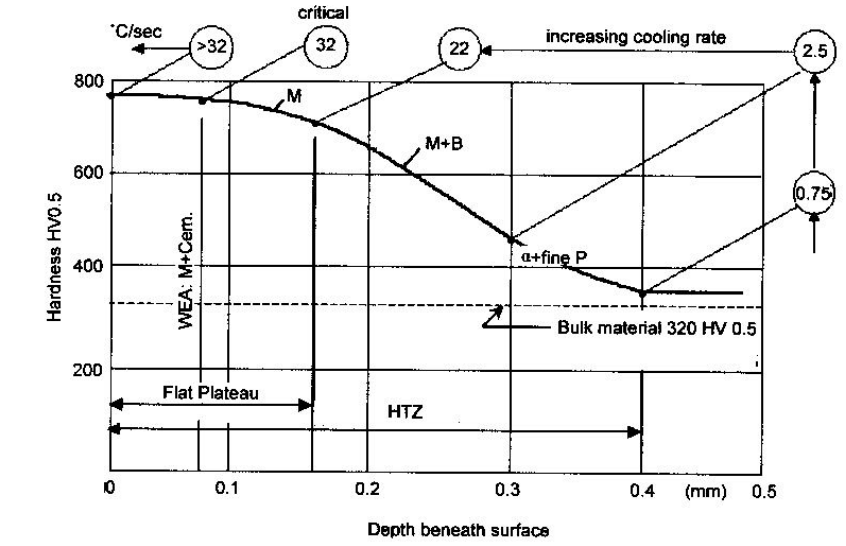


critical

| Cooling Curve* | 1st | 2nd | 3rd | 5th | 8th | Bulk Material |
|---|---|---|---|---|---|---|
| Cooling rate °C/s | > 32 | 32 | 22 | 2.5 | 0.75 | |
| HV 0.5 | > 750 | 750 | 650 | 440 | 350 → | 320 |
| RC | > 60 | 60 | 54 | 44 | 36 → | 33 |
| Micro-Structure | WEA M+Cem. | M | M + B | α + fine P | Tempered 42CrMo4 | |
| Depth µm | 60 | 150 | 300 | 400 | | |

Flat Plateau

HTZ

M = Martensite
B = Bainite
P = Pearlite
Cem. = Cementite

Fig. 10-a. Cooling rates and expected microstructure of tempered 42*CrMo*4, based on hardness distribution according to [4], and TTT-diagram in fig. 8-a.

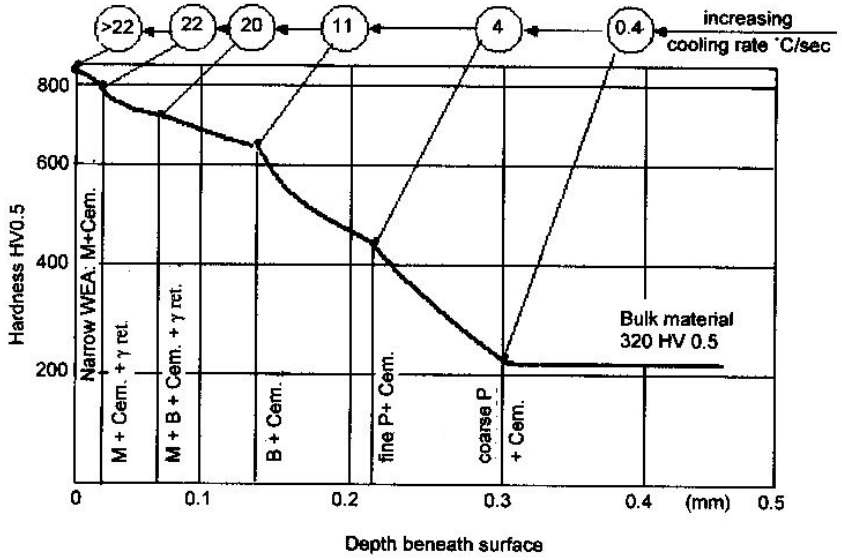


| Cooling Curve* | 1st - 3rd | 4th | - | 5th 7th | 8th 10th | Bulk material |
|---|---|---|---|---|---|---|
| Cooling rate °C/s | > 22 | 22 | 20 | 11 4 | 2 0.4 | |
| HV 0.5 | > 800 | 800 | 720 | 630 454 | 339 289 | → 237 |
| RC | > 62 | 62 | 58 | 55 45 | 35 29 | → 23 |
| Micro-Structure | M+ Cem. | M+Cem. + γ ret. | +M+B +Cem. + γ ret. | B + Cem. | fine P + Cem. coarse P + Cem. | annealed 100 Cr 6 |
| Depth µm | 20 | 60 | 140 | 220 | 300 | |

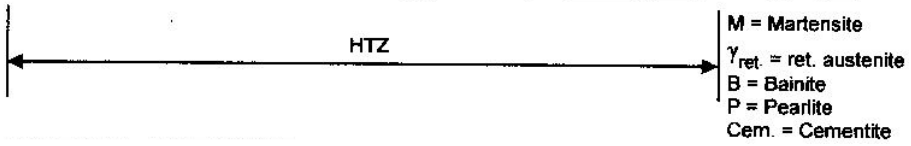


Fig. 10-b. Cooling rates and expected microstructure of annealed 100 *Cr6* based on hardness distribution according to [4], and TTT diagram in fig. 8-b.

- Low alloy hypo-eutecoid steels, are recommended for Grind-Hardening, since in this case minimum amount of austenite is retained during martensitic transformation.
- Brinksmeier and Brockhoff [11], assessed the whole HTZ as a zone of martensitic phase transformation, which is not altogether correct, as previously explained under 2.2.2.

**Acknowledgement**

The authors would like to express their gratitude for the fruitful mutual discussions with Prof. A. El-Ashram concerning some metallurgical affairs related to the topics dealt with in this paper.

**References**

[1] H.K. Tönshoff, et al., "Grinding Process Achievements and their Consequences on Machine Tools Challenges and Opportunities", Annals of the CIRP, Vol. 47 (2) (1998).

[2] M.C. Shaw and A. Vyas, "Heat-Affected Zones in Grinding Steel", Annals of the CIRP, Vol. 43 (1), pp. 279-282 (1994).

[3] R. Snoyes, M. Maris, I. Perers, "Thermally Induced Damage in Grinding", CIRP Annals 27 (2), pp. 571-581 (1978).

[4] S. Malkin, "Grinding Technology-Theory of Machining with Abrasives", Ellis Horwood, Chichester, UK (1989).
[5] W. Littman W. Wulff, J., "Heating and Cooling rates Work Surafce During of Bearing Steel, Trans, ASTME Vol. 47, pp. 692-714 (1955).
[6] K. Wagner, "Das Schleifen, Ein Ungewolltes Verfahren Der Oberflächen Wärme-Behandlung", Härterei-Technique and Wärmebehandlung, Vol. 3, pp. 83-85 (1957).
[7] E. Brinksmeier and T. Brockhoff, "Randschicht-Wärmebehandlung Durch Schleifen", HTW, Vol. 49, pp. 327-330 (1994).
[8] E. Brinksmeier, et al., "Friction, Cooling, and Lubrication in Grinding", Annals of the CIRP, Vol. 48 (2) (1999).
[9] E. Brinksmeier, "Grind-Hardening: A Comprehensive View", Annals of the CIRP, Vol. 48 (1) (1999).
[10] E. Brinksmeier and T. Brockhoff, "Advanced Grinding Processes for Surface Strengthening of Structural Parts", Technical Communication, Machining Science and Technology, Vol. 1 (2), pp. 299-309 (1997).
[11] E. Brinksmeier, "Utilization of Grinding Heat as a New Heat Treatment Process", Annals of the CIRP, Vol. 45 (1) (1996).
[12] C.A. Keyser, Basic Engineering Metallurgy, Printice-Hall 2nd Edition (1959).
[13] Y. Lakhtin, Engineering Physical Metallurgy", MIR-Publ., 3rd Edition, (1968).
[14] E.C. Rollason, "Metallurgy for Engineers", Edward Arnold Pub., London (1961).
[15] C. Guo and S. Malkin, "Analytical and Experimental Investigation of Burnout in Creep Feed Grinding", Annals of the CIRP, Vol. 43 (1) (1994).
[16] C. Guo, et al., "Temperatures and Energy Partition for Grinding with Vitrified Wheels", Annals of the CIRP, Vol. 48 (1) (1999).
[17] Z. Nishiyama, Martensitic Transfor-Mation, Acad. Press (1978).
[18] L.H. Van Vlock, Materials Science For Engineers, Addison Wesley Pub. Co (1970).
[19] S. Malkin and R.B. Anderson, Thermal Aspects of Grinding-Part 1 – Energy Partition, J. of Engineering for Ind., Nov. (1974).
[20] W. König and J. Messer, "Influence of the Composition and Structure of Steels on Grinding Process", Annals of the CIRP, Vol. 30 (2) (1981).
[21] F. Weber, et al., "Atlas Zur Wärmebehandlung Der Stähle", Düsseldorf (1958).

Received January 16, 2006
Accepted March 30, 2006